HHS Public Access

Author manuscript

Am J Med Genet A. Author manuscript; available in PMC 2021 May 20.

Published in final edited form as:

Am J Med Genet A. 2020 July ; 182(7): 1796–1800. doi:10.1002/ajmg.a.61614.

Spondyloepimetaphyseal dysplasia with elevated plasma lysosomal enzymes caused by homozygous variant in *MBTPS1*

Daniel R. Carvalho[1], **Carlos E. Speck-Martins**[1], **Jaime M. Brum**[1], **Carlos R. Ferreira**[2], **Nara L. M. Sobreira**[3]

[1]SARAH Network of Rehabilitation Hospitals, Brasilia, Brazil [2]Medical Genomics and Metabolic Genetics Branch, National Human Genome Research Institute, National Institutes of Health, Bethesda, Maryland [3]McKusick-Nathans Department of Genetic Medicine, Johns Hopkins School of Medicine, Baltimore, Maryland

Abstract

Variants in *MBTPS1* (membrane-bound transcription factor peptidase, site 1) encoding the protein convertase site-1 protease (S1P) were recently reported in a single individual with skeletal dysplasia and elevated plasma lysosomal enzymes. Here, we report the second individual with this newly described autosomal recessive spondyloepiphyseal dysplasia (OMIM #618392), presenting severe growth retardation, cataract and dysmorphic features, mainly retromicrognathia. Epilepsy and craniosynostosis were novel findings in our proband. She was found to be homozygous for a novel nonsense variant p.Trp983Ter in *MBTPS1*. In addition, she had normal levels of lysosomal enzyme activity in leukocytes but elevated levels in plasma. Our description confirms the existence of this new skeletal dysplasia and expands the phenotype and genotype of the disease.

Keywords

cataract; *MBTPS1*; retromicrognathia; site-1 protease (S1P); spondylepimetaphyseal dysplasia

Correspondence Daniel R. Carvalho, SARAH Rehabilitation Hospital, Setor Medico Hospitalar Sul, Quadra 501, Conjunto A, Brasilia-DF, 70335-901, Brazil, drochacarvalho@gmail.com, Nara L. M. Sobreira, McKusick-Nathans Department of Genetic Medicine, Johns Hopkins University School of Medicine, 733 North Broadway Street, Suite 569, Baltimore, MD 21205, nsobrei2@jhmi.edu.

AUTHOR CONTRIBUTIONS

Research clinic activities were conducted by D.R.C. and C.E.S.M. Lysosomal enzyme activity measurement were coordinated by J.M.B. Genetic analysis and clinical data interpretation were performed by D. R.C., C.R.F., and N.L.M.S. Figures, table and manuscript draft were conducted by D.R.C., C.R.F., and N.L.M.S. All co-authors contributed to review and approval of final manuscript.

CONFLICT OF INTEREST

The authors declare no conflict of interest.

DATA AVAILABILITY STATEMENT

Data sharing is not applicable to this article as no new data were created or analyzed in this study.

SUPPORTING INFORMATION

Additional supporting information may be found online in the Supporting Information section at the end of this article.

1 | INTRODUCTION

To date, only one affected individual has been found to harbor compound heterozygous pathogenic variants in *MBTPS1* associated with a spondyloepiphyseal dysplasia (OMIM #618392). The authors described an individual manifesting severely retarded growth with skeletal abnormalities, bilateral cataract, dysmorphic facial features, normal cognitive profile, and elevated plasma lysosomal enzymes (Kondo et al., 2018).

MBTPS1 (membrane-bound transcription factor peptidase, site 1) encodes site-1 protease (S1P). Kondo et al. (2018) showed by that S1P deficiency causes partial impairment of mannose-6-phosphate-dependent Golgi-to-lysosome transport of lysosomal enzymes. One secondary effect of this defective M6P-dependent delivery to lysosomes was the increased levels of plasma lysosomal enzymes detected in the proband (Kondo et al., 2018).

Here, we report a 5-year-old Brazilian girl with a very similar phenotype, including elevated plasma lysosomal enzymes, and a homozygous nonsense variant in *MBTPS1*. To the best of our knowledge, she represents the second individual with this disease; thus, our description supports the existence of this new autosomal recessive skeletal disorder.

2 | RESULTS

The family was recruited from the SARAH Network of Rehabilitation Hospitals as part of the Baylor-Hopkins Center for Mendelian Genomics (BHCMG) project. The study was approved by the local Institutional Ethics Committee (CAAE 26974619.0.0000.0022) and by the Johns Hopkins Medicine Institutional Review Board. Written informed consent was obtained for the use of pictures and clinical findings.

2.1 | Clinical report

Our proband is the second daughter of a healthy consanguineous couple (second degree cousins). The mother was 37 years old and the father 50 years old at the time of her birth. Her healthy sister is 22 years old.

After an uneventful pregnancy, the child was born preterm (34 weeks of gestation) and her weight was 1,970 g (Fenton Z-score −0.38), length 41 cm (Fenton Z-score −1.13), and OFC 31 cm (Fenton Z-score 0.24). At 36 months of age, she presented short stature with rhizomelic limb shortening and severe retromicrognathia (Figure 1). Her length was 68 cm (CDC −7.3 SD), weight was 7.6 kg (CDC −7.0 SD) and OFC was 46.5 cm (CDC −1.3 SD).

She developed congenital lamellar cataract and underwent surgical lens removal at age 10 months. Given hepatomegaly with increased hepatic transaminase, she received ursodeoxycholic acid until 30 months of age. There was no manifestation of emesis, food intolerance, fracture or luxation. Hearing was normal.

Motor milestones were delayed. Head control was obtained at 10 months and she sat at 16 months of age. She walked around 24 months and spoke her first words around 26 months. To date, at age 5 years and 8 months, she has not had sphincter control. Although receptive language is preserved, expressive language is delayed, and, to date, she has about 10 words.

She has had generalized seizures since 10 months of age. During the last semester, she has had clonic seizures weekly even under three different anticonvulsant drugs. Electroencephalogram showed generalized distribution of spike and polyspike discharges, at times followed by slow waves and complex high voltage spike-waves of 2–3 Hz.

Skeletal radiographs revealed diffuse osteopenia, small and irregular epiphyses of tubular bones, mildly enlarged and irregular metaphyses, ovoid lumbar vertebral bodies and a copper beaten skull (Figure 2 and Supplementary Figure S1). Computed tomography (CT) of the head at 37 months of age revealed early closure of coronal and sagittal sutures (Supplementary Figure S2). She did not present signs of intracranial hypertension, so neurosurgical intervention was not indicated.

Brain CT and MRI, brainstem auditory evoked response, electroneuromyography, echocardiogram, and renal ultrasound were normal.

Chromosome microarray analysis was normal. The following biochemical tests did not reveal abnormal values: alkaline phosphatase, parathyroid hormone, serum calcium, phosphorus, magnesium, vitamin D, venous blood gas, ammonia, lactate, urea, creatinine, cystatin C, alpha-feto protein, creatine phosphokinase, prothrombin time, and blood cell count. Normal metabolic tests included urine organic acid analysis, phytanic acid and very long chain fatty acids concentration and transferrin isoelectric focusing.

However, six lysosomal enzymes had increased activities in plasma, but had normal activity in leukocytes (Table 1).

At age 5 years and 8 months, height was 79 cm (CDC −6.9 SD), arm span was 77 cm, weight was 9 kg (CDC −8.8 SD), OFC was 47.5 cm (<3rd percentile), chest circumference was 50 cm, and nipple distance was 11.5 cm. She presented severe short stature with kyphosis, pectus carinatum, and dysmorphic facial features. She had a large forehead, prominent cheekbones, marked retromicrognathia, thick lips, and large ears (Figure 1). Hands and feet were normal. Skin, hair, teeth, and nails were normal. Hernias were not detected.

2.2 | Whole exome sequencing (WES) and variant analysis

WES was performed on the proband and her parents utilizing genomic DNA extract from blood. Libraries were sequenced on the NovaSeq 6000 platform using 100 bp paired end runs and NovaSeq 6000 S2 Reagent Kit and standard workflow. Fastq files were aligned with BWA mem (Li 2013) version 0.7.15 to the 1000 genomes phase 2 (GRCh37) human genome reference. Duplicate molecules were flagged with Picard version 2.17.0. Base call quality score recalibration and binning (2, 10, 20, and 30) were performed using the Genome Analysis Toolkit (GATK) (McKenna et al., 2010) version v4.0.1.1. Cram files were generated using SAMTools version 1.7. GATK's reference confidence model workflow was used to perform joint sample genotyping using GATK version 3.7. Variant filtering was done using the Variant Quality Score Recalibration (VQSR) method (DePristo et al., 2011). For SNVs, the annotations of MQRankSum, QD, FS, ReadPosRankSum, MQ, and SOR were used in the adaptive error model. HapMap3.3, Omni2.5, and 1000G phase high confidence

snp calls were used as training sites with HapMap3.3 and Omni2.5 used as the truth set. SNVs were filtered to obtain all variants up to the 99.9th percentile of truth sites (0.1% false negative rate). For indels, the annotations of FS, ReadPosRankSum, MQRankSum, QD, and SOR were used in the adaptive error model (4 max Gaussians allowed). A set of curated indels obtained from the GATK resource bundle (Mills_and_1000G_gold_standard.indels.b37.vcf) were used as training and truth sites. Indels were filtered to obtain all variants up to the 99.9th percentile of truth sites (0.1% false negative rate). Single sample .vcf files were created from the multi-sample .vcf file in order to be able to distribute the data by family and perform filtering by individual. Variants that passed VQSR filtering were annotated using Annovar (version 2013_09_11) against a variety of data sources.

Using the PhenoDB Variant Analysis Tool (Sobreira et al., 2015), heterozygous, homozygous, and compound heterozygous rare (minor allele frequency <1%) functional variants (missense, nonsense, stop loss, splice site variants, and indels) were prioritized in the proband. We identified a novel homozygous nonsense variant in *MBTPS1* (NM_003791.2; exon 22; c.2948G>A: p.Trp983ter) in the proband that was heterozygous in each of the unaffected parents.

This variant is not reported either in the 1000 Genomes Project, Exome Variant Server database, Exome Aggregation Consortium (ExAC) database, or in the Genome Aggregation Database (gnomAD). This nonsense variant c.2948G>A causes a termination codon that is located within 50 bp of the last intron-exon boundary, and is predicted to escape nonsense-mediated mRNA decay (NMD) (Supplementary Figure S3).

We validated this variant by Sanger sequencing in the proband and confirmed that the unaffected parents were each heterozygous. We also found that the unaffected sister was heterozygous for this pathogenic variant.

Further analysis of this family's WES data did not identify any additional potential variant that could account for the novel clinical features of epilepsy and craniosynostosis.

3 | DISCUSSION

Skeletal dysplasias represent a large and heterogenous group of diseases, most of which are rare. A nosology has been recently updated with delineation of new clinical entities and genes and pathways that are associated with skeletal dysplasias (Mortier et al., 2019). The *MBTPS1* gene that encodes site-1 protease (S1P) was not included in this nosology, but *MBTPS2* that encodes site-2 protease (S2P) was included in the Osteogenesis Imperfecta (OI) and decreased bone density group as Osteoporosis-X-linked form, OI type XIX (OMIM #301014) (Lindert et al., 2016). Our report supports the existence of this spondyloepimetaphyseal dysplasia caused by pathogenic loss-of-function (LoF) variants in *MBTPS1* and characterized by severe growth deficit, osteopenia, cataract, retromicrognathia, and elevated plasma lysosomal enzymes. It is important to note the similarity of the features in the two probands with LoF *MBTPS1* variants, mainly the

spondyloepiphyseal changes and dysmorphic facial features with marked retromicrognathia (Kondo et al., 2018).

There are few reports of phenotypes related to *MBTPS1*. One study described heterozygous missense variant (de novo) in the transmembrane domain of S1P (p.Pro1003Ser) in an adult proband with episodic hyperCKemia and focal myoedema (Schweitzer et al., 2019), a phenotype markedly different from our proband. The different phenotype could be due to a gain-of-function caused by the *MBTPS1*-p. Pro1003Ser variant instead of a LoF like in our proband.

Site-1 protease is expressed in the Golgi where it functions sequentially with the S2P to proteolytically activate unique membrane-bound latent transcription factors. It was suggested that S1P function is required for skeletal development, mainly in secretory cells such as osteoblasts and chondrocytes. S1P is a critical protease for activating various membrane-bound transcription factors that induce physiological endoplasmic reticulum (ER) stress, necessary to increase protein folding and secretory capacities. One hypothesis linking S1P deficiency to bone disease is impaired unfolded protein response (UPR) during normal skeletal development (Kondo et al., 2018; Saito et al., 2009).

The second hypothesis is that S1P deficiency causes abnormal secretion of lysosomal enzymes due to impairment of mannose-6-phosphate-dependent delivery to lysosomes. This could lead to extracellular matrix degradation due to abnormally secreted lysosomal enzymes with collagenase activity (Kondo et al., 2018). However, the skeletal manifestations of S1P deficiency are markedly different from those of mucolipidosis, caused by a deficiency of GlcNAc phosphotransferase (alpha/beta subunits encoded by *GNPTAB*, gamma subunit encoded by *GNPTG*), and also associated with mistargeting of lysosomal enzymes (Marschner et al., 2011). As in the previously reported case, we found normal lysosomal enzyme activities in leukocytes and markedly increased plasma enzyme activities (Kondo et al., 2018). This represents functional evidence of pathogenicity of the detected variant, since the S1P cleaves the alpha/beta precursor encoded by *GNPTAB* into its active and discrete alpha and beta subunits, which are needed for synthesis of the mannose-6-phosphate tag that targets enzymes to the lysosomes. The mistargeted enzymes in S1P deficiency and in mucolipidosis are thus instead secreted to the extracellular space.

Although S1P and S2P share most substrates and LoF mutations in these genes are related to skeletal dysplasia conditions, the clinical manifestations of these disorders are different, indicating distinct function of these regulatory proteases.

Comparing the clinical features, we noted that epilepsy and craniosynostosis were not present in the previous clinical case report (Kondo et al., 2018). In the absence of any other variant that could explain these features and considering the role of S1P as a regulatory protease in other tissues, we suggest that these clinical manifestations might be part of S1P deficiency phenotype. The developmental delay noted in our report could be associated to epilepsy that has not been controlled yet.

In conclusion, our report describes a novel homozygous *MBTPS1* pathogenic variant causing a phenotype that is very similar to a previous description of a new

spondyloepimetaphyseal dysplasia characterized by severe growth deficit, cataract, retromicrognathia and elevated plasma lysosomal enzymes.

Supplementary Material

Refer to Web version on PubMed Central for supplementary material.

ACKNOWLEDGMENTS

We sincerely thank the family members for their participation and their permission to publish the clinical data. The authors are grateful to all professionals of SARAH Brasilia Hospital by the assistance with our proband and support for data interpretation. The work was funded in part by the Baylor-Hopkins Center for Mendelian Genomics (NHGRI UM1 HG006542).

Funding information

National Human Genome Research Institute, Grant/Award Number: UM1 HG006542

REFERENCES

DePristo M, Banks E, Poplin R, Garimella K, Maguire J, Hartl C, … Daly M (2011). A framework for variation discovery and genotyping using next-generation DNA sequencing data. Nature Genetics, 43, 491–498. [PubMed: 21478889]

Kondo Y, Fu J, Wang H, Hoover C, McDaniel JM, Steet R, … Xia L (2018). Site-1 protease deficiency causes human skeletal dysplasia due to defective inter-organelle protein trafficking. JCI Insight, 3(14), e121596.

Lindert U, Cabral WA, Ausavarat S, Tongkobpetch S, Ludin K, Barnes AM, … Shotelersuk V (2016). MBTPS2 mutations cause defective regulated intramembrane proteolysis in X-linked osteogenesis imperfecta. Nature Communication, 7, 11920.

Li H (2013). Aligning sequence reads, clone sequences and assembly contigs with BWA-MEM. arXiv:1303.3997v1 [q-bio.GN].

Marschner K, Kollmann K, Schweizer M, Braulke T, & Pohl S (2011). A key enzyme in the biogenesis of lysosomes is a protease that regulates cholesterol metabolism. Science, 333, 87–90. [PubMed: 21719679]

McKenna A, Hanna M, Banks E, Sivachenko A, Cibulskis K, Kernytsky A, … DePristo MA (2010). The genome analysis toolkit: A MapReduce framework for analyzing next-generation DNA sequencing data. Genome Research, 20, 1297–1303. [PubMed: 20644199]

Mortier GR, Cohn DH, Cormier-Daire V, Hall C, Krakow D, Mundlos S, … Warman ML (2019). Nosology and classification of genetic skeletal disorders: 2019 revision. The American Journal of Medical Genetics: Part A, 179(12), 2393–2419.

Saito A, Hino S, Murakami T, Kanemoto S, Kondo S, Saitoh M, … Imaizumi K (2009). Regulation of endoplasmic reticulum stress response by a BBF2H7-mediated Sec23a pathway is essential for chondrogenesis. Nature Cell Biology, 11(10), 1197–1204. [PubMed: 19767744]

Schweitzer GG, Gan C, Bucelli RC, Wegner D, Schmidt RE, Shinawi M, … Brookheart RT (2019). A mutation in site-1 protease is associated with a complex phenotype that includes episodic hyperCKemia and focal myoedema. Molecular Genetics & Genomic Medicine, 7(7), e00733.

Shapira E, Blitzer MG, Miller J, & Africk DK (1989). Biochemical genetics: A laboratory manual (p. 145). New York, Oxford: Oxford University Press.

Sobreira N, Schiettecatte F, Boehm C, Valle D, & Hamosh A (2015). New tools for Mendelian disease gene identification: PhenoDB variant analysis module; and GeneMatcher, a web-based tool for linking investigators with an interest in the same gene. Human Mutatation, 36(4), 425–431.

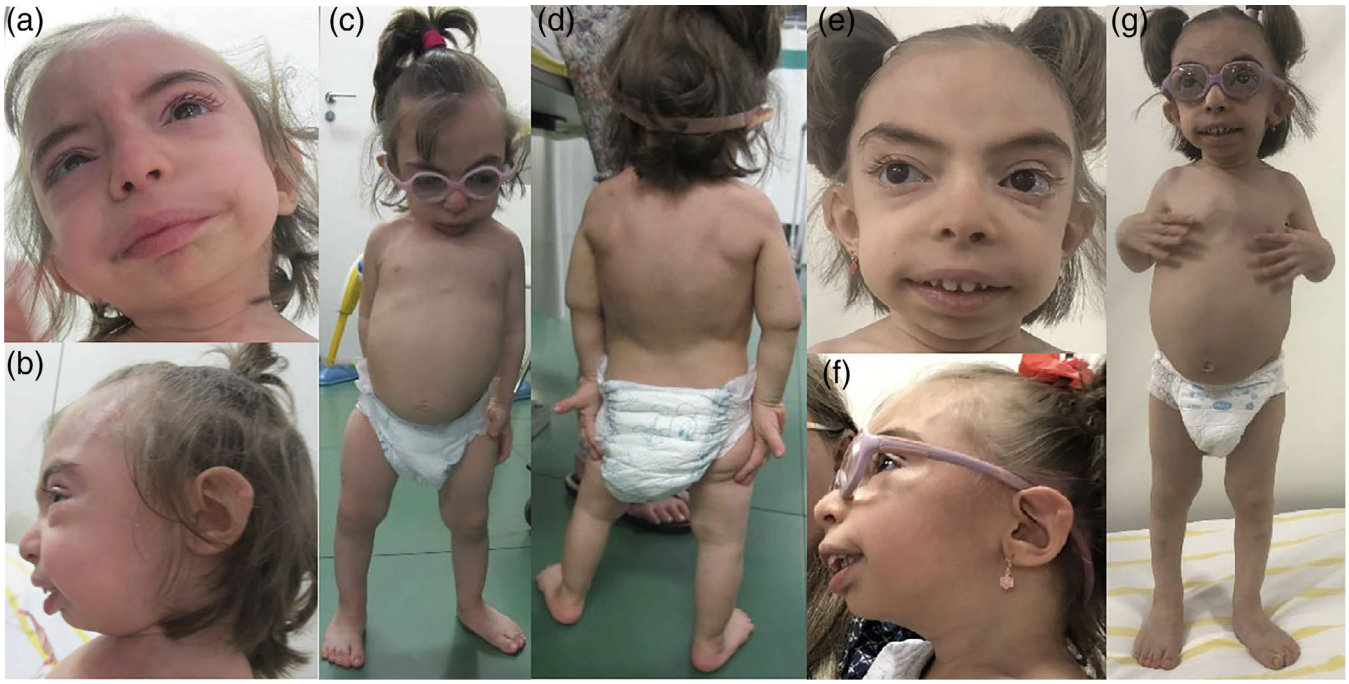

FIGURE 1.

Clinical pictures at age of (a–d) 40 months and (e–g) 68 months. Note coarse face with severe retromicrognathia, thick and prominent lips, wide mouth commissure, broad forehead with thick and salient supraorbital region, and protruding external ears. Other features include short neck, pectus carinatum, large and protruding abdomen, shortening of limbs (more evident in upper extremities), but normal aspect of hands and feet [Color figure can be viewed at wileyonlinelibrary.com]

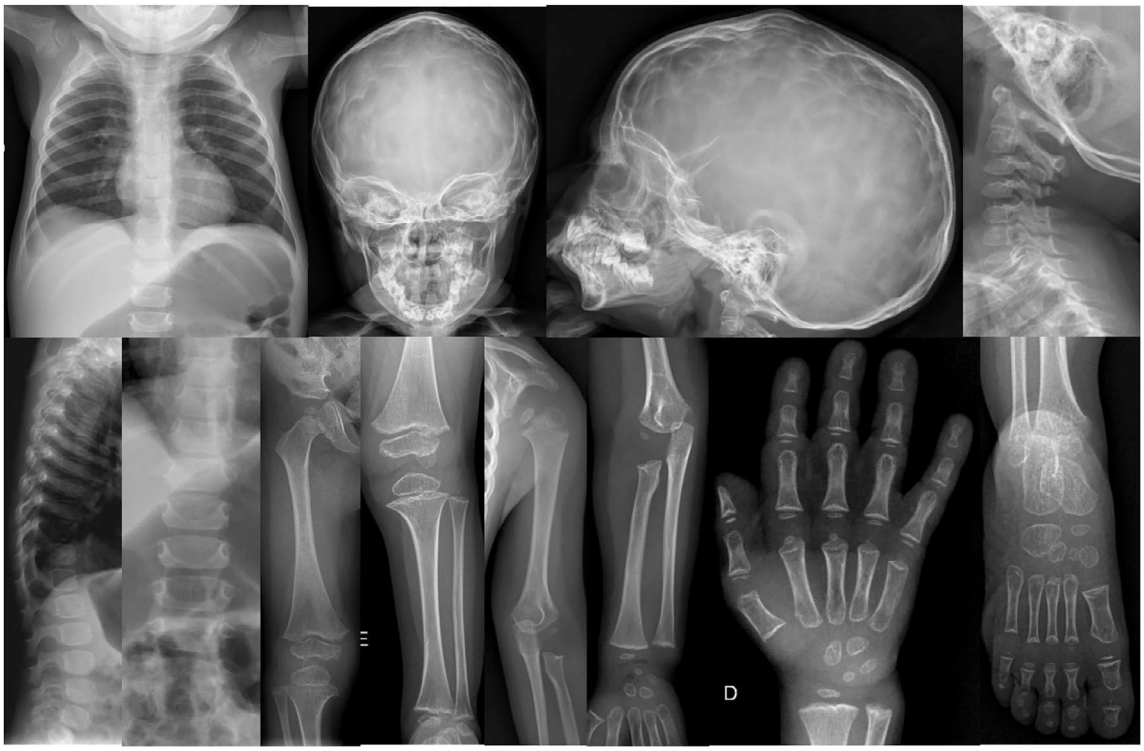

FIGURE 2.

Radiographies at age of 37 months. Note diffuse osteopenia, ovoid aspect of lumbar vertebral bodies, irregular aspect of cervical vertebral bodies with mild reduction of height dimension, metaphyseal and epiphyseal irregularities of long bones, mild metaphyseal enlargement, small tubular bone epiphysis, and copper beaten skull

TABLE 1

Activity of lysosomal enzymes in patient and reference range

Enzyme	Leukocytes	Plasma	Reference range
Total beta-hexosaminidases		3,975	400–1,400 nmol/h/ml
Alpha-N-acetylglucosaminidase		39	9–32 nmol/h/ml
Iduronate-2-sulfatase		1,080	167–475 nmol/4 h/ml
Alpha-N-acetylgalactosaminidase		648	60–240 nmol/17 h/ml
Hexosaminidase A (MUGS substrate)		109	20–51 nmol/h/ml
Beta-glucuronidase	195	3.49	300–500 nmol/h/mg and 1.0–3.0 nmol/h/ml
Beta-galactosidase	608		410–1,600 nmol/h/mg
Arylsulfatase A	492		320–1,200 nmol/h/mg
Alpha-mannosidase	613		400–1,000 nmol/h/mg
Alpha-iduronidase	7		2–12 nmol/h/mg
Alpha-fucosidase	146		100–300 nmol/h/mg

Note: Assay methodology: Shapira et al. (1989).

Am J Med Genet A. Author manuscript; available in PMC 2021 May 20.